RATE CONTROL MECHANISM IN SOLID STATE DECARBURIZATION OF FERROMANGANESE

P.J. Bhonde[1] and R.D. Angal[2]

[1]Western Regional Instrumentation Centre, University of Mumbai, Vidyanagari, Kalina Campus, C.S.T. Road, Santacruz (East), Mumbai, Pin Code- 400 098, India
E-mail: pbhondeus@yahoo.com
[2]Department of Metallurgical Engineering & Material Sciences, Indian Institute of Technology, Powai, Mumbai, Pin Code - 400 076, India. E-mail: ramchandraangal@yahoo.co.in

ABSTRACT

Conventionally low carbon ferromanganese is manufactured globally by refining high carbon ferromanganese in liquid state. This process is an expensive and lengthy technique. Hence, the present work was undertaken with the objective of understanding the feasibility and kinetics of the solid state refining of ferromanganese. The process involved transformation of carbon rich carbides viz. Mn_3C_2, Mn_7C_3 into metal rich carbide i.e. $Mn_{15}C_4$, $Mn_{23}C_6$ by subjecting the alloy powder to a flowing stream of carbon dioxide.

Effect of the process governing parameters such as time, temperature, particle size, pressure on the extent of decarburization was studied. Without any loss of manganese in the form of fumes or slag, it was observed that, there was substantial reduction, viz. 65 per cent in the total carbon content, by this technique. Subsequently, the process was investigated to find out the mechanism of carbon removal.

Depending upon the temperature and the particle size, it was found that the rate controlling mechanism changes from chemical reaction control to product layer (ash) diffusion control. The activation energy for each of the aforesaid mechanism was computed. The values thus obtained substantiated the aforesaid mechanisms.

1. INTRODUCTION

Production of low-carbon ferromanganese is a multi-stage, multi-furnace, eco-polluting, energy intensive and low yield process. This escalates the low carbon ferromanganese price. However, high-carbon ferromanganese, in which manganese is present as carbon rich carbide acts as an economic source of manganese [1]. In steel making, it is predominantly used for introducing manganese into the steel, which improves desirable mechanical properties of alloy steel [2-3].

Presence of carbon in alloy steel, primarily originating from high-carbon ferromanganese, subsequently leads to its failure due to phenomena *viz.* 'sensitization, weld decay [4].' The present investigation hence aimed at studying the feasibility of solid-state removal of carbon from its parent source, *i.e.* high-carbon ferromanganese. Attempts were also made to understand the rate controlling mechanism of the overall process.

In industries 'High Temperature Oxidation' of alloys in carbon containing gases is normally a major problem. Here this fact is used in a positive way to design a practical technique for making low-carbon ferromanganese [5]. It works on the principle of transformation of carbon rich carbides from high-carbon ferromanganese to metal rich carbides. The chosen alloy was subjected to oxidizing environment containing the flowing stream of carbon dioxide under isobaric, isothermal condition for various intervals of time.

Proceedings: Tenth International Ferroalloys Congress; 1 – 4 February 2004
INFACON X: '*Transformation through Technology*' Cape Town, South Africa
ISBN: 0-9584663-5-1 Produced by: Document Transformation Technologies

Even kinetically slow, *i.e.* solid-solid homogeneous reactions, between different solid oxidizers such as MnO_2, $MnCO_3$ and pulverized ferromanganese were attempted to enhance the grade of the final product.

However the overall rate was improved by siphoning out CO generated according to the following reaction

$$1/6 \langle Mn_{23}C_6 \rangle + \langle MnO \rangle \rightarrow 29/6 \langle Mn \rangle + (CO) \quad (1)$$

$$\Delta G^o = 325.82 - 0.18\ T \quad kJ.$$

Earlier studies of oxidation behavior of ferromanganese alloy indicated activation energy for diffusion of Mn^{++} to be 130 kJ/mole[6]. Oxidation kinetics was found to obey 'parabolic law' of oxidation. The rate controlling mechanism was diffusion of Mn^{++} through the metal matrix. Oxidation of carbon will occur only when, carbon diffuses through the metal matrix. Further, it should react with the oxidizer at the metal-gas interfaces. Being a heterogeneous reaction, it is obvious that such an oxidation is associated with certain mechanism in which reaction takes place in successive steps. In the present work attempts have been made to have insight of the prevailing reaction mechanism.

2. EXPERIMENTATION

The experimental set-up consisted of resistance heating furnace capable of reaching 1473 K. Main reaction chamber consisted of an impervious, recrystallised alumina tube. Both the open ends were sealed with indigenously fabricated couplings of stainless steel of AISI 316. They had provision for gas inlet and outlet ports. The chamber was evacuated up to 10^{-6} torr by operating combination of rotary and diffusion pump. Vacuum level was monitored with combined digital pirani-penning gauge. A calibrated K type chromel-alumel thermocouple was used as a temperature sensor. Reactants as well as products were subjected to material characterization studies. These involved elemental analysis by Strohlein apparatus, XRD for phase identification, metallography with optical microscopy and EDAX-SEM for microanalysis of the phases.

The experimental procedure adopted for the sample preparation for studying the decarburization of ferromanganese has been cited earlier [7]. The current work incorporated the same procedure with only difference that, regular geometry alloy powder compacts replaced the regular geometry cast samples in the earlier work. Two average particle sizes of 98 μm and 48 μm with close distribution and spherical shape were used for making the compacts. The compacts were not sintered. But they had sufficient strength to withstand the handling stresses.

3. RESULTS AND DISCUSSION

An attempt was made to correlate the fitting of the outcome of the investigation with the usual heterogeneous non-catalytic kinetics model viz. Unreacted Core Shrinking Model [8-10]. Purpose of such study was to find out the prevailing rate controlling mechanism of the process [11]. For mathematical simplicity a single particle decarburization was considered which could be further extrapolated and generalized [12]. Shape factor for the particle was taken unity assuming complete spheroids. Although fine grains yielded considerable quantum of decarburization, for kinetic studies compacts were made from particles having average size *viz.* 49 and 98 μm respectively.

The extent of decarburization was monitored by estimating the change in mass and carbon content of the compact at different temperatures and at different times. For comparative studies exposure periods were maintained the same. Figure 1 shows that, the decarburization of specimens exposed to a CO_2 current at 1323 K was restricted only to a small depth of the surface. For solid deoxidizer *viz.* MnO_2, the decarburization depth was found to be much larger as indicated in the figure 2.

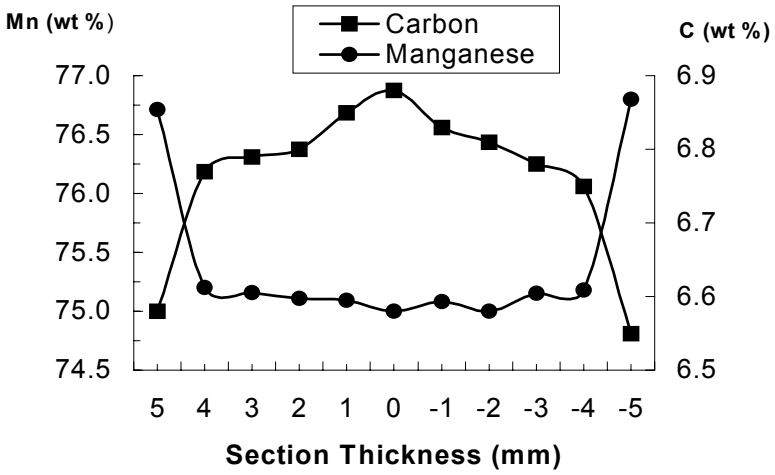

Figure 1. Effect of gaseous deoxidizer on the extent of decarburization.

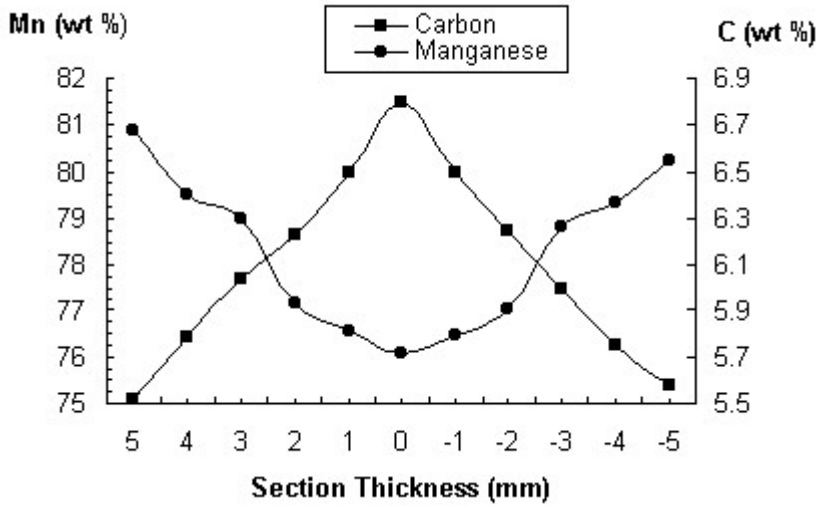

Figure 2. Effect of solid deoxidizer on the extent of decarburization.

Instead of full conversion only the fractional decarburization of the alloy was computed which was based on the results of performed experiments for a selected set of parameters. In external gaseous oxidizer method, the solid-state decarburization process can be divided into following steps [13] occurring sequentially.

- Diffusion of CO_2 through the film surrounding the ferromanganese particle to the surface of solid.
- Penetration and diffusion of CO_2 through the blanket (ash) on the surface of the unreacted core.
- Chemical reaction of CO_2 at the interface leading to formation of various carbides and oxides [14-15].
- Outward diffusion of carbon and the product gas *i.e.* CO, from the ash layer back to the exterior surface of the layer of ferromanganese particle.
- Diffusion of the product gas in through the gas film back into the main stream of CO_2.

Overall, the rate of a reaction is the ratio of driving force of and net resistance to the reaction. In the present investigation, the process being irreversible, steps number IV and V do not directly contribute to the reaction rate. Also the magnitude of the resistance offered by each step varies and the one contributing highest resistance may be the rate-controlling step. In this treatment as shown in the equation (2) to (4), the fractional conversion parameters [16] for the first three steps were used to study the reaction mechanism.

Film diffusion control parameter — $t/\tau = X_B$ (2)

Ash Diffusion Control parameter — $t/\tau = 1- 3(1-X_B)^{2/3} + 2(1- X_B)$ (3)

Chemical reaction control parameter — $t/\tau = 1 - (1-X_B)^{1/3}$ (4)

Where,

X_B = fractional conversion in terms of quantity of carbon
B = reactant solid
t = time in s corresponding to X_B
τ = time for complete conversion of the alloy particle

During decarburization by externally supplied CO_2, the compacted specimen undergoes formation of the ash layer encapsulating the inner unreacted core of alloy, which gradually shrinks with the exposure time. Fractional conversions were calculated for the different rate control mechanisms. Calculations involved made use of the carbon depletion data for the high-carbon ferromanganese compacts made from the alloy particles of average size of 98 μm. These compacts were decarburized under the experimental conditions. Based on this information and from equations (2) to (4), the fractional time for the corresponding rate control mechanism were determined. However, the figures 3 to 5 represent the functional plots of the variation of the fractional conversion versus time under the given experimental conditions.

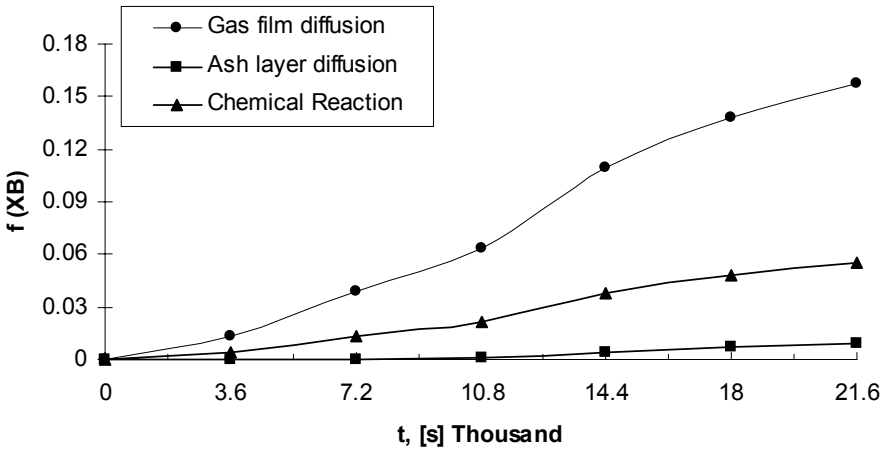

Figure 3. Isothermal reaction rate data at 1273 K for 98 μm alloy.

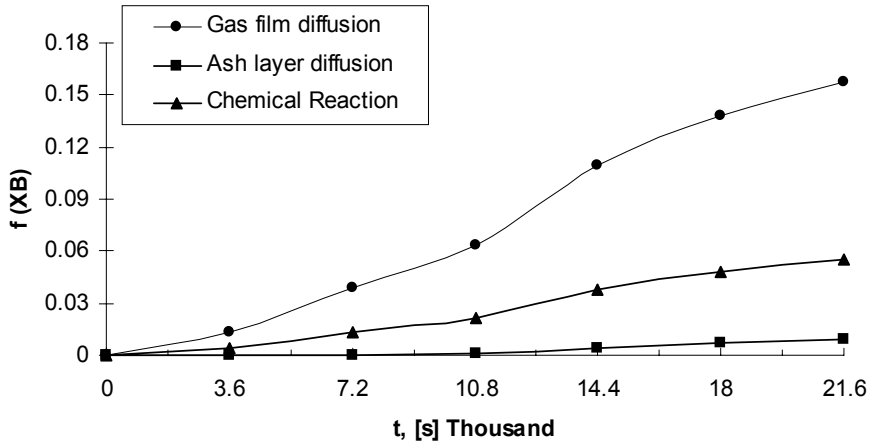

Figure 4. Isothermal reaction rate data at 1323 K for 98 μm alloy.

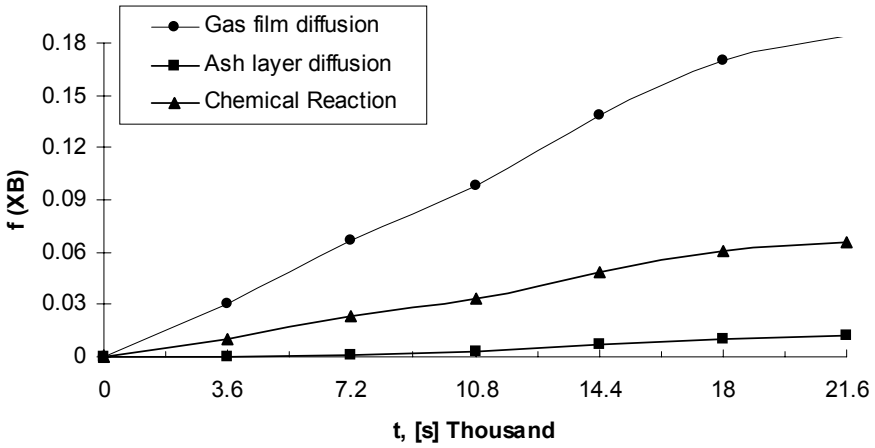

Figure 5. Isothermal reaction rate data at 1373 K for 98 μm alloy.

Effect of particle size was studied by carrying out similar studies on compacts made from 49, 69 and 388 μm particles respectively. However, for comparison purposes, the isothermal reaction rate data of compacts prepared from finer particles, 49 μm is graphically represented in the figures 6 to 8. Based upon the equations (2) to (4), and the values of the slopes for the respective best-fit lines for appropriate control mechanism, the ratio of slopes for two different particle sizes is related by:

$(CS_1/CS_2) = (R_2/R_1)$ — for chemical reaction control (5)

$(AS_1/AS_2) = (R_2/R_1)^2$ — for ash layer diffusion control (6)

Where,

CS_1, CS_2, AS_1, AS_2 = slope of the linear fit of the reduced time plot at Temperature T_1 for chemical reaction, ash layer diffusion control for particles of radius R_2 and R_1 respectively.

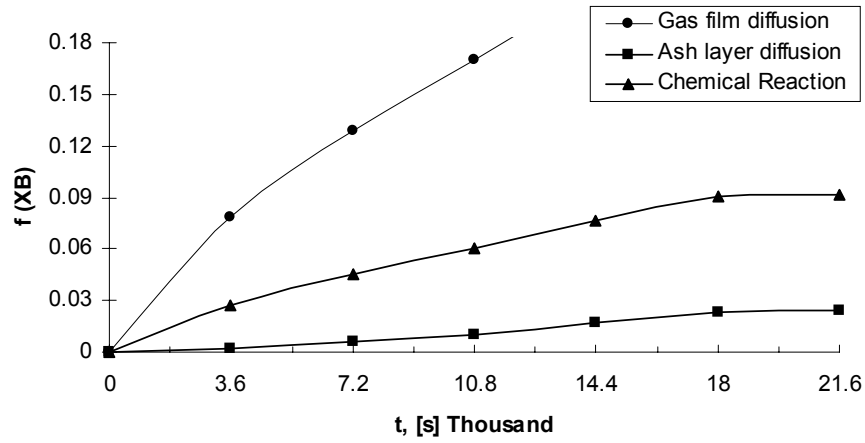

Figure 6. Isothermal reaction rate data at 1273 K for 49 μm alloy.

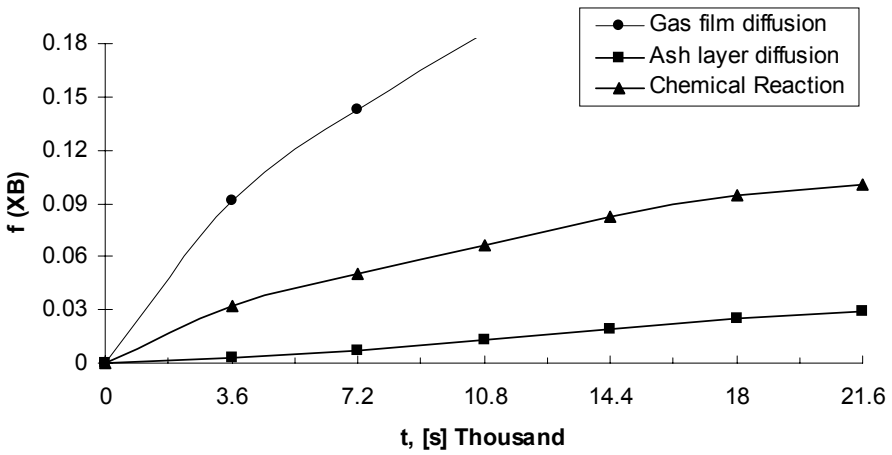

Figure 7. Isothermal reaction rate data at 1323 K for 49 μm alloy.

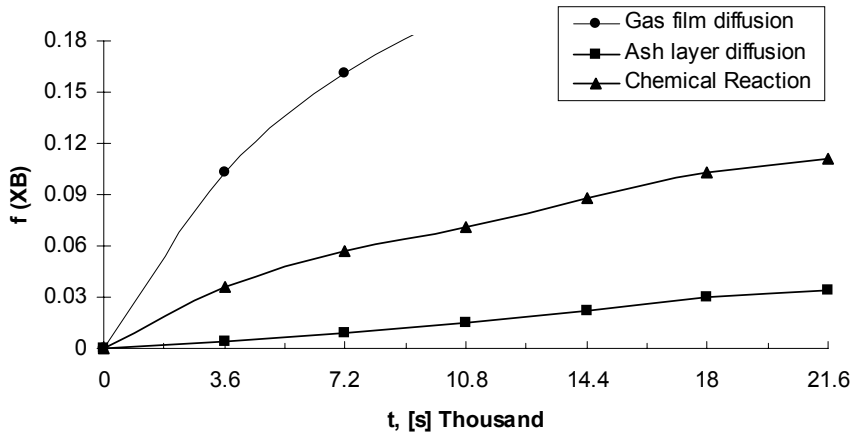

Figure 8. Isothermal reaction rate data at 1373 K for 49 μm alloy.

From the figures 3 to 5 it was observed, that only at 1273 K, the best linear relationship between fractional conversion and time was found for chemical control equation (4). It thus implies that, during the solid-state decarburization of the alloy compact made from coarse grains, the chemical reaction control may be the prevailing mechanism at low temperature and short durations. Mathematically, it was found that the fixed fractional conversion data obtained under isothermal condition for compacts made from various particle sizes of the alloy powder behaved in a linear manner. Magnitude of the ratio of slopes for two different particle sizes was found to be two. It confirmed that, the time needed for fractional conversion is directly proportional to the particle size but this is only true for the process governed by the chemical reaction control mechanism.

Functional plots of variation of fractional conversion of the isothermal reaction rate data for 49 μm alloy particles are illustrated in figures 6 to 8. It shows that, only at 1373 K, the best linear fit was for equation (3). This indicates a possibility of ash diffusion control mechanism under those conditions.

According to the earlier discussion, it is known that high-carbon ferromanganese particle gradually gets converted into the metal rich carbides and oxides surrounding a carbon rich carbides core. The ash layer consisting of metal rich carbides plus metal oxides encapsulates this core, the size of which diminishes with time. In the present investigation one of the reactants together with one of the products is a gaseous oxide. During the process they diffuse in a counter current direction through the ash layer. The ash layer, the thickness of which increases with time, offers higher impedance for mass transport. X-ray diffraction and optical microscopy studies of the decarburized sample have revealed the formation of mixed carbides and

oxides of the metal. From the data depicted in figure 6 to 8, it can be said that, there is a possibility of ash diffusion control mechanism [17] prevailing for fine grain material exposed for longer durations at high temperatures.

Mathematically the magnitude of the ratio of slopes for two different particle sizes was found to be four. This value justifies the possibility that diffusion of reacting or product species through the ash layer is the rate-controlling step [18-21] of the decarburization process.

It can thus be said that at low temperature, for a coarse grain compact the chemical reaction control may be the rate- controlling mechanism. On the other hand, for fine grains at higher temperatures the process may be under ash diffusion control. Therefore,the overall rate of solid-state decarburization of high-carbon ferromanganese may be the ratio of driving potential and the combination of the resistance offered by the individual reactions occurring in succession.

Normally the activation energy for interstitial diffusion in the stoichiometric binary oxides is of the order of 80 kJ/mole.

The diffusivity of carbon is enhanced [22] due to

- solubility of carbon in MnO lattice
- formation of cluster of MnO along with carbon.

Considering these facts, it is expected that the activation energy for diffusion of carbon in the MnO lattice would be small. The value of 45 - 61 kJ obtained in the present investigation can hence be justified.

For ash diffusion control mechanism, the slope AS_1 at temperature T_1 is given by -

$$[1 - 3 (1-X_B)^{1/3} + 2 (1-X_B)] / t = 1/ \tau = AS_1 \quad (7)$$

Hence substituting the value of τ the above equation becomes

$$[1 - 3 (1-X_B)^{1/3} + 2 (1-X_B)] / t = (\xi_B \times R_p^2) / (6 \times b \times D \times C_{Ag}) = AS_1 \quad (8)$$

$$D = D_o \times e^{(-Q/RT_1)} \quad (9)$$

Where,

b = coefficient of stoichiometry
C_{Ag} = concentration of reactant gas A
D = diffusion coefficient of gaseous reactant in ash layer
D_o = Pre-exponential constant.
Q = Activation energy kJ
R = ideal gas law constant
ξ_B = density of solid reactant B
T = Reaction temperature
R_p= Radius of alloy particle

From the equations (8) and (9), the slope AS_1 can be given by -

$$[\xi_B \times R_p^2] / [6 \times b \times D_o \times e^{(-Q/RT_1)} \times C_{Ag}] = AS_1 \quad (10)$$

Similarly at higher temperature T_2 the slope AS_2 for the same mechanism under identical experimental conditions will be given by equation (11).

$$[\xi_B \times R_p^2] / [6 \times b \times D_o \times e^{(-Q/RT_2)} \times C_{Ag}] = AS_2 \quad (11)$$

For identical values of ξ_B, R_p, D_o and C_{Ag}, the ratio of slopes over a range of temperatures can be calculated according to

$$\ln (AS1/AS2) = e^{[-Q(T2-T1)/RT1T2]} \quad (12)$$

However, the same equation (12) will hold good for any other control mechanism except the natural logarithm of the ratio of the slopes of the best fitting straight lines obtained under identical conditions would be for the respective control mechanism equation. Therefore, in case of a chemical reaction control mechanism, the activation energy can be calculated in similar way by substituting the value of τ in terms of $k_{s,}$ which is a first order rate constant for solid reaction. Thus mathematically the activation energy for a given process control mechanism is independent of particle size and density of the reactant, operating temperature and reacting gas pressure.

Logarithmic plot of k_s and D calculated at different temperatures against the reciprocal of the operation temperature gave the activation energy graphs as shown in figures 9 and 10 respectively. The activation energy for a chemical reaction control mechanism for the temperature range of 1273 to 1373 K was calculated. From figure 9, for 49 μm diameter particle the activation energy value was found to be 23.73 kJ. On the other hand, for 98 μm diameter particle it was 34.88 kJ.

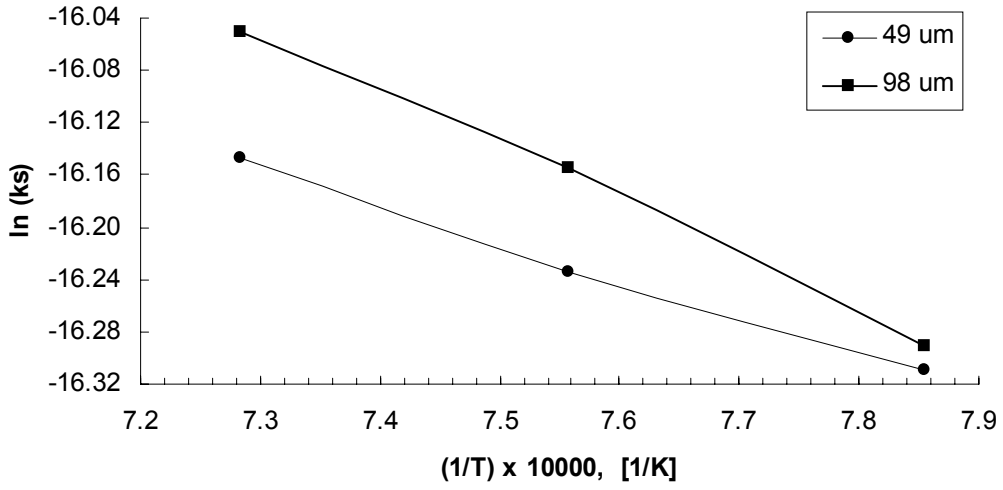

Figure 9. Activation energy plot for chemical reaction control.

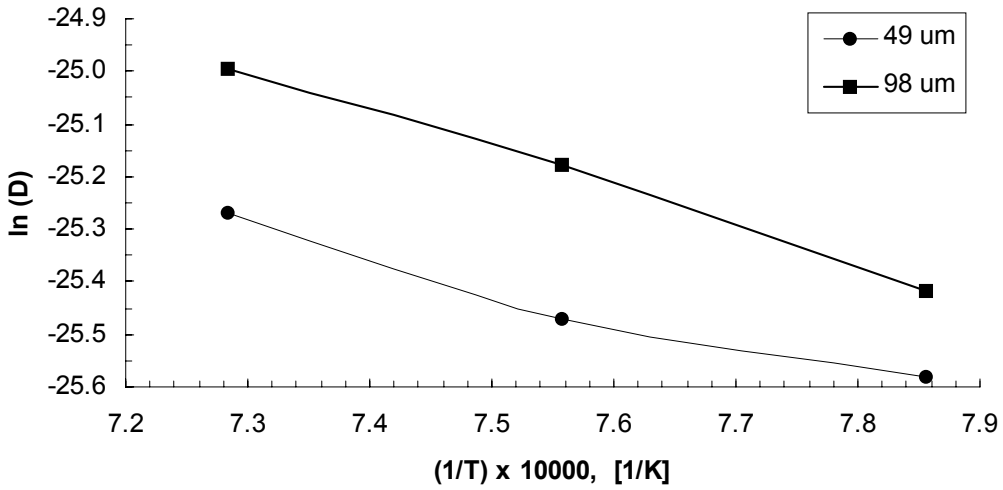

Figure 10. Activation energy plot for ash layer diffusion control.

The difference in the values of the activation energy may be ascribed to the variation in the dimension of the interface available for the chemical species to contact and react. In case of fine grain compact, the reacting species can short circuit through the larger low impedance zone, *i.e*. interact chemically on a comparatively wider interface. Overcoming this barrier is reflected in smaller magnitude of the activation energy.

Similarly, in the present investigation, as shown in figure 10, the activation energy for ash diffusion control mechanism in the temperature range 1273 to 1373 K for 49 μm particle size was found to be 45.05 kJ. However, for 98 μm diameter particle under symmetrical experimental conditions the activation energy value was found to be 61.19 kJ. This difference in the values may be attributed to the possible variation in the dimension of the pores of the compacts.

For two different particle sizes under identical conditions, the difference in magnitude of activation energy indicates a shift in control mechanism from chemical control to ash diffusion control with decreasing grain size of alloy. This also confirms earlier observation made.

Overall, it was found that the activation energy for ash diffusion control mechanism is nearly double that for the chemical reaction control mechanism, thereby indicating that if ash diffusing control mechanism prevails, the process will require larger energy for equivalent quantum of fractional decarburization.

4. CONCLUSIONS

Solid-state decarburization by external deoxidizer is a non-traditional, eco-friendly, energy-cost saving, process. It can be inferred that, at low temperature, for coarse grain compact the chemical reaction control may be the rate controlling mechanism. But in the case of fine grains at higher temperature the process may be under ash diffusion control.

The activation energy for a given process control mechanism is independent of particle size and density of the reactant, operating temperature and reacting gas pressure.

In case of fine grain compact, the reacting species can short circuit through the larger low impedance zone *i.e*. interact chemically on a comparatively wider interface. Overcoming of this barrier is reflected by the smaller magnitude of the activation energy value.

For two different particle sizes under identical conditions, the difference in magnitude of activation energy indicates a shift in control mechanism from chemical control to ash diffusion control with decreasing grain size of alloy.

Overall, it was found that the activation energy for ash diffusion control mechanism is nearly double that for the chemical reaction control, thereby indicating that if ash diffusing control mechanism prevails, the process will require larger energy for equivalent quantum of fractional decarburization.

5. REFERENCES

[1] Elyutin, V.P., Pavlov, Yu. A., Levin, B.E., Alekseev, E.M.: Production of Ferroalloys and Electrometallurgy, Editor: Geller, I. & Staff, Translator: Shapira, B., 2nd Edn., The State Scientific and Technical Publication House, Moscow, (1962), pp 96 - 137, 195.

[2] Kozak, D.S., Matricardi, L.R.: "Production of Refined Ferromanganese Alloy by Oxygen - Refining of High carbon Ferromanganese," 38th Electric Furnace, Conference Proceedings, Vol. 38, (1981), p 123.

[3] Barcza, N.A., Stewart, A.B.: "The Potential of Plasma Arc Technology for the Production of Ferroalloys," Proceedings of the 3 rd International Conference on Ferroalloys, Tokyo, Japan (1983), pp 1 - 24.

[4] Fontana, M.G., Green, N.D.: Corrosion Engineering, 2nd Edn., McGraw International Book Co., New York, (1978), pp 59 - 60.

[5] Schoukens, A.F.S., Curr, T.R.: "The Production of Manganese Ferro-alloy in Transferred-arc Plasma System," Proceedings of the 42nd Electric Furnace Conference, 4th – 7th Dec., 1984, Edward Brothers Inc., Michigan, (1985), pp 161 - 171.

[6] Upadhaya, G.S., Dube, R.K.: Problems in Metallurgical Thermodynamics and Kinetics, 1st Edn., Pergamon Press Ltd., Oxford, England, (1977), pp 221 - 224.
[7] Bhonde, P.J., Angal, R.D.: "Solid-state Decarburization of High-carbon Ferromanganese," Proceedings of the 6th International Ferroalloy Congress, Vol. I, 8th – 10th Mar., 1992, Cape Town, South Africa, MINTEK Pub., Randburg, Republic of South Africa, (1992), pp 161 - 165.
[8] Ray, H.S.: "The Use of Reduced Time Plots on Preliminary Identification of Reaction Mechanism," Trans. Ind. Inst.of Metals, Vol.36,(1983),pp 11-19.
[9] Beretka, J.: "Kinetic Analysis of Solid-state Reactants," J. Amer. Ceram. Soc., Vol. 67, (1984), pp 615 - 620.
[10] Szekely, J., Evans, J.W., Brimacombe, J.K. : The Mathematical and Physical Modeling of Primary Metal Processing Operations, 1st Edn., John Wiley & Sons Publication, New York, (1987), pp 13,31,133 – 145.
[11] Sohn, H.Y., Szekely, J.: Gas-solid Reactions, 1st Edn., Academic Press, New York, (1976), pp 176 - 177.
[12] Ray, H.S.: Kinetics of Metallurgical Reactions, 1st Edn., Oxford & IBH Publishing Co. Pvt. Ltd., New Delhi, (1993), pp 73 - 84.
[13] Levenspiel, O.: Chemical Reaction Engineering, 2nd Edn., Wiley Eastern Ltd., New Delhi, (1982), pp 357-376.
[14] Rao, Y.K., Jalan, B.P.: "A study of the Rates of Carbon-Carbon Dioxide Reactions in the Temperature Ranges 839°, 1050° C," Metall. Trans., Vol. 3 (B), Sept., (1972), pp 2465 - 2477.
[15] Sohn, H.Y., Szekely, J.: "Reactions Between Solids Through Gaseous Intermediate - I; Reactions Controlled by Chemical Kinetics," Chem. Engrg. Sci., Vol. 28, (1973), pp 1789 - 1801.
[16] Geiss, E.A.: "Equations and Tables for Analyzing Solid-state Reaction Kinetics," J. Amer. Ceram. Soc. Vol. 46, (1963), pp 374 - 376.
[17] El-Guindy, M.I., Davenport, W.G.: "Kinetics of Ilmenite Reduction with Graphite," Metall. Trans., Vol. 1, Jun., (1970), pp 1729 - 1734.
[18] Rama Rao, G.A., Venugopal, V., Sood, D.D.: "Kinetics and Mechanism of the Oxidation of ZrC," 9th International Symposium Thermal Analysis, Goa, 8th – 10th Nov., 1993,Goa University, (1993), pp 497 - 500.
[19] Weber, P., Eric, R.H.: ``The Reduction of hromite in the Presence of a Silica Flux," Metall. Trans. Vol. 24 (B), Dec., (1993), pp 987 - 995.
[20] Ghosh, A.: "Kinetics Studies in Process Metallurgy," Proceedings of the International Conference Thermodynamics and Kinetics of Metallurgical Processes, Bangalore, 15th – 18th Jul., (1981), pp 161 - 183.
[21] Akdogan, G., Eric, R.H.: "Kinetics of the Solid-state Carbothermic Reduction of Wessel Manganese Ores," Metallurgical and Materials Transactions, Vol. 26 (B), Feb., (1995), pp 13 - 24.
[22] Kofstad, P: "CO + CO_2 Mixture and Diffusion Transport in MnO," Oxidation of Metals, Vol. 19, No. 3/4, (1983), pp 129 - 149.